RSC Advances

This article can be cited before page numbers have been issued, to do this please use: J. W. Yang, H. Zhu, Y. L. Huang, W. Huang and W. Wang, *RSC Adv.*, 2016, DOI: 10.1039/C6RA22677A.

ROYAL SOCIETY OF CHEMISTRY

www.rsc.org/advances

View Article Online
DOI: 10.1039/C6RA22677A

Journal Name

COMMUNICATION

Design and Synthesis of Extended Quinoxaline Derivativesis and Their Charge Transport Properties

Received 00th January 20xx,
Accepted 00th January 20xx

DOI: 10.1039/x0xx00000x

www.rsc.org/

Junwei Yang, Haoyun Zhu, Yuli Huang, Wei Huang and Weizhi Wang*

A scalable and convenient strategy is described to synthesize conjugation extended quinoxaline derivatives from phenylene-ethynylene arrays. By tuning the solvent, the compounds are brightly emissive with an emission solvatochromism. Furthermore, the fabricated FET devices possess nice performance, whose mobilities are 0.47 $cm^2 V^{-1} s^{-1}$ and 0.99 $cm^2 V^{-1} s^{-1}$, respectively. The mobilities are higher than those of the alkyl substituted corresponding compounds, which can be proved by the grazing incidence X-ray diffraction (GIXRD) measurement.

Heterocyclic polycyclic aromatic hydrocarbons (hetero-PAHs) have attracted increasing attention in their design, synthesis as well as applications because of some fascinating features, such as high stability, low energy absorption, and high charge carrier mobility.[1] Among enormous N-substituted heterocycles that are pervasive in natural products, biologically active agents[2] and part structures in functional π-systems,[3] quinoxalines are extraordinarily attractive.[4] Many derivatives have been proven to possess in vitro antiparasitic activities,[5] anti-tumor activities,[6] and used as 5-HT3 receptors,[7] kinase inhibitors.[8] In addition, quinoxalines have also been applied as building blocks for the development of semiconducting materials,[9] fluorescent probes,[10] sensors,[11] anion receptors[12] and cavitands.[13] In general, the reaction features the condensation of 1,2-diamines with diketones to afford quinoxaline derivatives.[14] Recently, one-pot strategy has been proposed to construct quinoxaline oligomers using expensive metal catalysts, which possesses tedious isolation procedures.[15]

Address here. The State Key Laboratory of Molecular Engineering of Polymers, Collaborative Innovation Center of Polymers and Polymer Composite Materials, Department of Macromolecular Science, Fudan University, Shanghai 200433, China.

E-mail: weizhiwang@fudan.edu.cn; Tel: +86021-65643836

†Electronic Supplementary Information (ESI) available: experimental section including materials, measurements and characterizations, devices fabrication and characterization; mass spectra, NMR data for new compounds, UV, PL and cyclic voltammetry spectra of compounds and CCDC reference number of 10b: 1499076. For ESI or other electronic format see DOI: 10.1039/x0xx00000x

Due to this consideration, series of conjugation extended quinoxalines are prepared, with the simple catalyst and facility isolation. Dicarbonyl derivatives, as intermediate products, have been obtained without much effort, which are useful building blocks capable of undergoing various chemical transformations.[16] Different π-conjugated phenylene-ethynylene arrays, as starting compounds, made a decision for the sequence of the conjugation chain of final products. The insertion of the electron-withdrawing quinoxalines on the phenylene-ethynelene backbone influences the electronic structures and various properties of the compounds. Alkyl chains (*n*-butyl) are introduced to the compounds to improve solubility.

Scheme 1. Synthetic Procedures of Compounds 5-12.

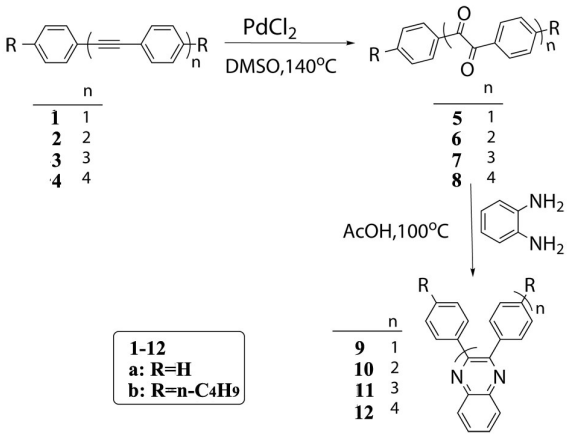

The oxidation of alkynes was catalyzed efficiently by $PdCl_2$ to afford intermediate products **5-8**, in which DMSO acted as a powerful oxidant (**Scheme 1**). The condensation reaction of compounds **5-8** and 1,2-phenylenediamine successfully afforded quinoxaline derivatives **9-12** in good yields, after plain filtration of **5-8**. Brunet products were avoided and white solids finally precipitated after these two separate steps. In our experimentation, the stepwise process was the key to obtain pure products in high yields, which was verified by ^{1}HNMR and

View Article Online
DOI: 10.1039/C6RA22677A

^{13}CNMR (**Fig. S1-S40**). With the increase of the π-conjugated skeleton, **11-12** are poorly soluble in acetic acid, leading to their nearly complete precipitation from the reaction mixture. The needle-like single crystal of **10b** was obtained by recrystallization from acetic acid. The X-ray analysis was conducted to establish the structure in **Fig. 1** and **Table S1**, which led to elucidation of its solid state structure.

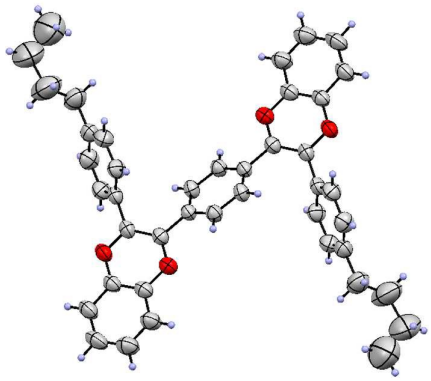

Fig. 1 The ORTEP drawing of **10b**.

The ultraviolet/visible (UV/vis) absorption and photoluminescence (PL) spectra of **9-12** in chloroform are shown in **Fig. S41, S42**, and the data is compared in **Table 1**. The extended structural unit affects the position of the absorption and emission band from 9 to 12, although the red-shift is not obvious. However, the electron-donating effect of n-butyl substituent results in a redshift of the longer wavelength absorption band to ca. 390 nm, which changes the electron cloud density of the adjacent benzene ring. In chloroform, compound **12b** emits deep blue photoluminescence with an emission maximum at 418 nm. However, the emission changes to bright green in acetone solutions. Depending on the variation of solvent, the result of the solvent polarity on the emission is quite positive and significant, ranging from 432 to 518 nm (**Fig. 2a**). The pronounced positive emission solvatochromism is additionally observable upon naked eyes, where the color changes from blue (toluene) to yellow-green (DMSO) (**Fig. 2a**). More polarizable solvent served to stabilize the excited state more than the ground state, which lessens the energy gap.[17] We also determined the photophysical of **12a** in same solvents and observed a similar bathochromic trend, exhibiting the PL emission maxima in the range from 480 to 525 nm (**Fig. 2b**).

Table 1. Photophysical Properties of compounds 9a-12a and 9b-12b.

Sample	UV[a]	PL[a]	Φ_F [a,b] (%)
9a	345	413	5.23
10a	358	416	10.35
11a	359	421	31.32
12a	359	425	54.37
9b	390	416	5.32
10b	394	417	11.24
11b	395	417	35.11
12b	396	418	62.33

[a] Absorption maximum in dilute $CHCl_3$ solutions. [b] Quantum yield estimated with quinine sulfate (Φ_F = 54% in 0.1 M H_2SO_4)

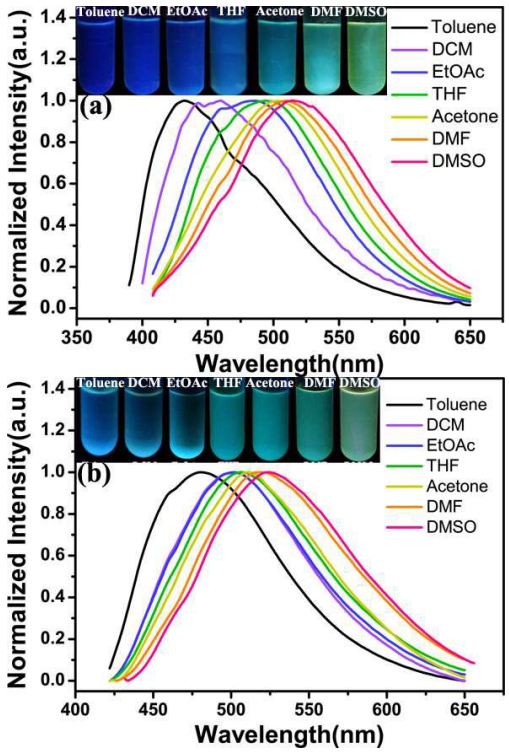

Fig. 2 Solvent-dependent emission spectra of (a) **12b** and (b) **12a**. Inset: the optical photograph of corresponding compounds in different solutions.

The introduction of an electron-donating or electron-accepting group directly affects the HOMO and LUMO levels of the compound. The cyclic voltammetry curves of quinoxaline derivatives **9-12** show no reversible peaks arising from the oxidation potential, which was ascribed to the electron-deficient pyrazine ring containing two sp^2-type centers (**Fig. S43**).[18] In the anodic scan, the onset of oxidation for **9a-12a** occurred at 1.06, 0.88, 0.75 and 0.70 V, which corresponded to HOMO values of -5.81,-5.63, -5.50 and -5.45 eV, respectively (**Table 2**). The oxidation potential values of alkylated oligomers follow the order **9b** > **10b** > **11b** > **12b**, which presents the same trend with the values of **9a-12a**. The extended conjugation length slightly raises the HOMO level and consequently reduces the band gap of the oligomers. The energy band gaps of **9a-12a** were calculated to be 3.28, 3.18, 3.15 and 3.12 eV, which were determined from the onset wavelength of their UV absorptions. The HOMO-LUMO energy gaps showed good correlations with their UV data and the molecular extended conjugation chain.

View Article Online
DOI: 10.1039/C6RA22677A

Table 2. Electrochemical Properties of compounds 9a-12a and 9b-12b.

Sample	E_{onset}^{ox}	HOMO	λ_{onset}	ΔE_g (eV)	LUMO
9a	1.06	-5.81	378	3.28	-2.53
10a	0.88	-5.63	389	3.18	-2.45
11a	0.75	-5.50	394	3.15	-2.35
12a	0.70	-5.45	397	3.12	-2.33
9b	0.96	-5.71	390	3.18	-2.53
10b	0.86	-5.61	395	3.14	-2.47
11b	0.73	-5.48	396	3.13	-2.35
12b	0.69	-5.44	398	3.12	-2.32

[a]Abbreviations: E_{onset}^{ox} is the onset potential for oxidation. HOMO is calculated by the equation: HOMO = − e(E_{onset}^{ox} − 0.0468 V) − 4.8 eV. λ_{onset} is the onset wavelength of UV absorptions. LUMO = ΔE_g + HOMO.

The transfer integral and reorganization energy, which are believed to be important for the mobility of semiconductors, are both extremely based on the arrangement of the organic molecules.[19] To further inspect and compare the molecular packing characteristics of quinoxaline derivatives with the extended skeleton, two-dimensional grazing incidence X-ray diffraction (2D-GIXRD) measurements were performed. As for oligomer **12a**, the clear (100) reflection arch appears along the q_z direction, with a q_z value of 11.2 nm^{-1} (**Fig. 3a**). Furthermore, a clear arch shape of the (010) diffraction peak in the in-plane direction appears at q_{xy}= 18.01 nm^{-1}, which corresponds to the π−π stacking distance of 3.49 Å. Obviously, **12a** tends to pack more orderly and tightly than **12b** in neat films, which may be due to the steric hindrance caused by alkyl chains. The obvious (010) arch of compound **12b** appears at q_{xy}= 17.50 nm^{-1}, whose π−π distance is 3.59 Å (**Fig. 3b**). Compared with the variation in π−π

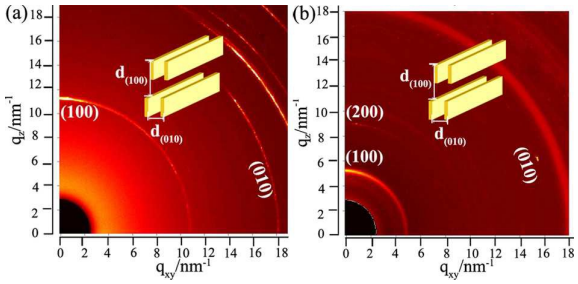

Fig. 3 The 2D-GIXRD pattern of (a) **12a** and (b) **12b**.

stacking, the alkyl substitute is of larger influence for the spacing in out-of-plane direction. The intense reflections of the (100) plane along the q_z (out-of-plane) and a relative weak (010) plane along q_{xy} (in-plane) axes of **12b** films can be observed from **Fig. 3b**, which implies that **12b** molecules would prefer to have the edge-on structure.[20] The ordered edge-on structure of organic molecules prefers to be formed in high performances FETs, which allows the molecules to arrange along the direction in the conducting channel and then get an efficient charge transport.[19] In addition, the decreased conjugated chain made some differences. Compared to **12a**, the out-of-plane spacing of **11a** increased to 5.66 Å, whose π−π stacking distance rose to 3.50 Å as well (**Fig. S44**).

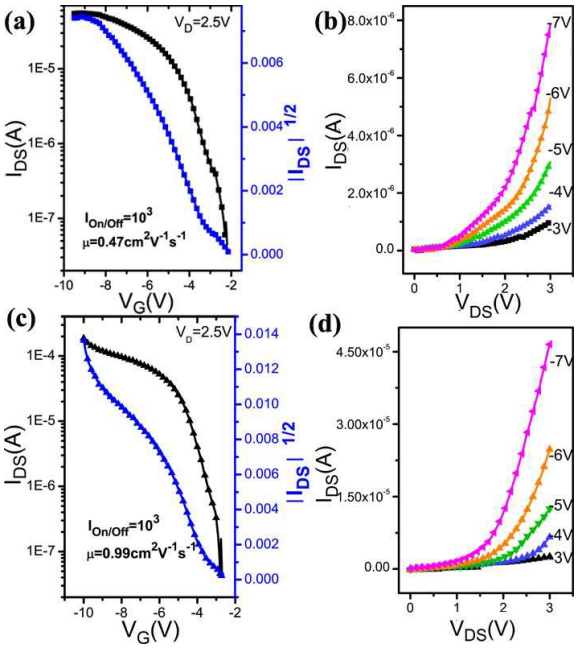

Fig. 4 (a) Transfer and (b) output characteristics of the **11a** devices (W = L = 1000 μm) at a drain source voltage (V_{DS}) = 2.5 V. (c) Transfer and (d) output characteristics of the **12a** based FETs.

The higher HOMO energy level suggests that **12** might have great potential for use in field-effect transistors (FETs) as p-type materials.[21] Furthermore, N-Heteroatoms provide a new method of tuning the intrinsic molecular electronic properties and improving stability, which have been extensively studied in organic thin film transistors.[22] Quinoxaline derivativesis **11a-12a** and **11b-12b** with high thermal stabilities are beneficial for the processing of the electrical devices (**Fig. S45**). We evaluated the charge transport properties of the oligomers **11a-12a** and **11b-12b** by fabricating field-effect transistors in the "top-contact top-gate" geometry. To this end, FETs using the quinoxaline derivatives were fabricated using ion gels[23] to efficiently diminish the heat generated at work and to endow low voltage operation.[24] Besides, the top-gated quinoxaline derivatives transistors prepared using ion gel gate dielectrics has been rarely reported. The representative transfer curve (I_D-V_G) of the FET with **11a** is displayed in **Fig. 4a** and that of the **12a** is shown in **Fig. 4c.** The best results of **11a** and **11b** devices exhibit mobilities up to 0.47 cm^2 V^{-1} s^{-1} and 0.44 cm^2 V^{-1} s^{-1}, respectively, with on/off ratios up to 10^3 (**Fig. S46**). While the significant increases of the mobilities were observed on the **12a**, **12b** based devices, 0.99 cm^2 V^{-1} s^{-1} and 0.88 cm^2 V^{-1} s^{-1} were respectively evaluated from the saturation regime (**Fig. S47**). In addition, the output characteristics (I_D-V_D) of the aluminum-gated quinoxaline derivatives based FETs at five different gate voltages (V_G), as shown in **Fig. 4b** and **Fig. 4d**, affirming the clear p-channel characteristics. The structure−property relationship has been verified by a range of analyses, especially using 2D-GIXRD. The substantial structural

View Article Online
DOI: 10.1039/C6RA22677A

change has an enormous influence on the packing of the neighboring molecules, which in turn affects the specific properties. The extended conjugated chain and the closer structures did have a great influence on the conductive properties according to the above comparisons. The mobility of **12** is among the best results ever reported on N-Heteroatoms.[25]

Conclusions

In summary, series of conjugation extended quinoxaline oligomers **9-12** have been successfully synthesized by a convenient and efficient route with the simple procedure of isolation. The compounds **12a** and **12b** display positive emission solvatochromism, as revealed by detailed optical studies. The performance of **11a** and **12a** based FET devices is comparable, showing mobilities of 0.47 $cm^2 V^{-1} s^{-1}$ for **11a** and 0.99 $cm^2 V^{-1} s^{-1}$ for **12a**. Furthermore, the FET fabricated with **11b** and **12b** is also measured, whose mobilities are lower than their corresponding molecules **11a** and **12a**, respectively. The employment of 2D-GIXRD provides a direct explanation for the difference in FET performance between **12a** and **12b**, in which the alkyl chain weakens the molecular packing.

Acknowledgment

This work was financially supported by the National Natural Science Foundation of China (21274027 and 20974022) and the Innovation Program of Shanghai Municipal Education Commission (15ZZ002). The FETs were fabricated and characterized in Fudan Nanofabrication Laboratory. The synchrotron-based 2D-GIXRD measurement was supported by Shanghai Synchrotron Radiation Facility (15ssrf00474).

Notes and references

1 (a) C. Wang, J. Zhang, G. Long, N. Aratani, H. Yamada, Y. Zhao, Q. Zhang, *Angew. Chem., Int. Ed.* 2015, ***54,*** 6292-6296. (b) C. Dou, S. Saito, K. Matsuo, I. Hisaki, S. Yamaguchi, *Angew. Chem., Int. Ed.* 2012, ***51***, 12206-12210.
2 M. Ishikura, T. Abe, T. Choshi, S. Hibino, *Nat. Prod. Rep.* 2013, ***30***, 694-752.
3 (a) T. Meyer, D. Ogermann, A. Pankrath, K. Kleinermanns, T. J. J. Müller, *J. Org. Chem.* 2012, ***77***, 3704-3715. (b) W. Chen, K. Tian, X. Song, Z. Zhang, K. Ye, G. Yu, Y. Wang, *Org. Lett.* 2015, ***17***, 6146-6149.
4 (a) T.-C. Chou, K.-C. Lin, M. Kon-no, C.-C. Lee, T. Shinmyozu, *Org. Lett.* 2011, ***13,*** 4588-4591. (b) J. A. Pereira, A. M. Pessoa, M. N. Cordeiro, R. Fernandes, C. Prudencio, J. P. Noronha, M. Vieira, *Eur. J. Med. Chem.* 2015, ***97***, 664-672.
5 (a) J. Guillon, E. Mouray, S. Moreau, C. Mullie, I. Forfar, V. Desplat, S. Belisle-Fabre, N. Pinaud, F. Ravanello, A. Le-Naour, J.-M. Leger, G. Gosmann, C. Jarry, G. Deleris, P. Sonnet, P. Grellier, *Eur. J. Med. Chem.* 2011, ***46***, 2310-2326.
6 (a) Q. Weng, D. Wang, P. Guo, L. Fang, Y. Hu, Q. He, B. Yang. *Eur. J. Pharmacol.* 2008, ***581***, 262-269. (b) D. Patrizia, M. Annamaria, B. Paola, M. Alessandra, D. Gaetano, C. Girolamo, D. Francesco, S. Alessia, V. Daniela, B. Giuseppe, V. Giampietro, *J. Med. Chem.* 2008, ***51***, 2387-2399.
7 S. Butini, R. Budriesi, M. Hamon, E. Morelli, S. Gemma, M. Brindisi, G. Borrelli, E. Novellino, I. Fiorini, P. Ioan, A. Chiarini, A. Cagnotto, T. Mennini, C. Fracasso, S. Caccia, G. Campiani, *J. Med. Chem.* 2009, ***52,*** 6946-6950.
8 C. Srinivas, C. N. S. S. P. Kumar, V. J. Rao,; S. Palaniappan, *J. Mol. Catal. A: Chem.* 2007, ***265***, 227-230.
9 (a) E. Wang, L. Hou, Z. Wang, S. Hellström, F. Zhang, O. Inganäs, M. R. Andersson, *Adv. Mater.* 2010, ***22***, 5240-5244. (b) Y. Wu, Z. Yin, J. Xiao, Y. Liu, F. Wei, K. J. Tan, C. Kloc, L. Huang, Q. Yan, F. Hu, H. Zhang, Q. Zhang, *ACS Appl. Mater. Interfaces* 2012, ***4***, 1883-1886. (c) D.-W. Chang, H.-J. Lee, J.-H. Kim, S.-Y. Park, S.-M. Park, L. Dai, J.-B. Baek, *Org. Lett.* 2011, ***13***, 3880-3883. (d) W. Chen, Q. Zhang, T. Salima, S. A. Ekahana, X. Wan, T. C. Sumd, Y. M. Lama, A. H. H. Cheng, Y. Chen, Q. Zhang, *Tetrahedron* 2014, ***70*** , 6217-6221
10 H. Liu, T. Duan, Z. Zhang, C. Xie, C. Ma, *Org. Lett.* 2015, ***17***, 2932-2935.
11 (a) G. Li, Y. Wu, J. Gao, J. Li, Y. Zhao, and Q. Zhang, *Chem. Asian J.* 2013, ***8***, 1574–1578. (b) P. Gu, Z. Wang and Q. Zhang, *J. Mater. Chem. B,* 2016, DOI: 10.1039/C6TB02052F.
12 (a) T. Kazunobu, O. Ryusuke, M. Tomohiro, *Chem. Commun.* 2002, 212. (b) Y. Qu, J. Hua, H. Tian, *Org. Lett.* 2010, ***12***, 3320-3323.
13 B. D. Lindner, Y. Zhang, S. Hofle, N. Berger, C. Teusch, M. Jesper, K. I. Hardcastle, X. Qian, U. Lemmer, A. Colsmann, U. H. F. Bunz, M. Hamburger, *J. Mater. Chem. C* 2013, ***1***, 5718-5724.
14 (a) D. Zhang, Y. Yang, M. Gao, W. Shu, L. Wu, Y. Zhu, A. Wu, *Tetrahedron* 2013, ***69***, 1849-1856. (b) Y. Xu, X. Wan, *Tetrahedron Lett.* 2013, ***54***, 642-645.
15 C. Mousset, O. Provot, A. Hamze, J. Bignon, J.-D. Brion, M. Alami, *Tetrahedron* 2008, ***64***, 4287-4294.
16 (a) S. K. Singh, V. Saibaba, V. Ravikumar, S. V. Rudrawar, P. Daga, C. S. Rao, V. Akhila, P. Hegde, Y. K. Rao, *Bioorg. Med. Chem.* 2004, ***12***, 1881-1893. (b) X. Deng, N. S. Mani, *Org. Lett.* 2006, ***8,*** 269-292.
17 S. Nigam, S. Rutan, *Appl. Spectrosc*. 2001, ***55***, 362A-370A.
18 H.-J. Son, W.-S. Han, K.-R. Wee, D.-H. Yoo, J.-H. Lee, S.-N. Kwon, J. Ko, S. O. Kang, *Org. Lett.* 2008, ***10***, 5401-5404.
19 C. Wang, H. Dong, W. Hu, Y. Liu, D. Zhu, *Chem. Rev.* 2012, ***112,*** 2208-2267.
20 Y. Qu, Q. Su, S. Li, G. Lu, X. Zhou, J. Zhang, Z. Chen, X. Yang, *ACS Macro Lett.* 2012, ***1***, 1274-1278.
21 (a) Q. Miao, *Adv. Mater.* 2014, ***26***, 5541-5549. (b) J. Li and Q. Zhang, *ACS Appl. Mater. Interfaces* 2015, ***7***, 28049−28062. (c) C. Wang, P. Gu, B. Hu and Q. Zhang, *J. Mater. Chem. C*, 2015, ***3***, 10055-10065.
22 S. Yang, B. Shan, X. Xu, Q. Miao, *Chemistry* 2016, ***22***, 6637-6642.
23 (a) H. Okamoto, R. Eguchi, S. Hamao, H. Goto, K. Gotoh, Y. Sakai, M. Izumi, Y. Takaguchi, S. Gohda, Y. Kubozono, *Sci. Rep.* 2014, ***4***, 5330. (b) T. Fujimoto, K. Awaga, *Phys. Chem. Chem. Phys.* 2013, ***15***, 8983-9006.
24 (a) B. J. Kim, H. Jang, S. K. Lee, B. H. Hong, J. H. Ahn, J. H. Cho, *Nano Lett.* 2010, ***10***, 3464-3466. (b) C. Zhang, Y. Zang, E. Gann, C. R. McNeill, X. Zhu, C.-A. Di, D. Zhu, *J. Am. Chem. Soc.* 2014, ***136***, 16176-16184.
25 (a) U. H. Bunz, J. U. Engelhart, B. D. Lindner, M. Schaffroth, *Angew. Chem., Int. Ed.* 2013, ***52***, 3810-3821. (b) Q. Miao, *Synlett* 2012, ***23***, 326-336.

View Article Online
DOI: 10.1039/C6RA22677A

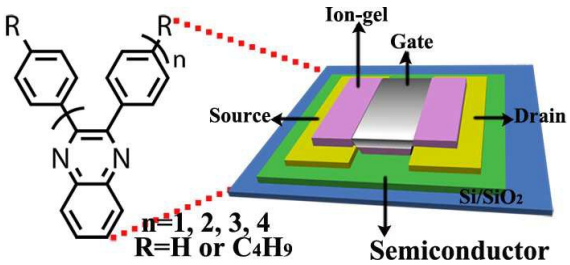

A scalable and convenient strategy is described to synthesize conjugation extended quinoxaline derivatives from phenylene-ethynylene arrays. The fabricated FET devices possess nice performance, whose mobilities are 0.47 $cm^2 V^{-1} s^{-1}$ and 0.99 $cm^2 V^{-1} s^{-1}$, respectively.